Earth Surface Processes and Landforms
Earth Surf. Process. Landforms **25**, 497–504 (2000)

RELATION OF SEDIMENT TRANSPORT CAPACITY TO STONE COVER AND SIZE IN RAIN-IMPACTED INTERRILL FLOW

ATHOL D. ABRAHAMS[1]*, PENG GAO[1] AND FRANK A. AEBLY[2]
[1]*Department of Geography, State University of New York at Buffalo, Buffalo, NY 14261, USA*
[2]*Michael Baker Corporation, 3601 Eisenhower Avenue, Suite 600, Alexandria, VA 22304, USA*

Received 8 March 1999; Revised 4 August 1999; Accepted 12 October 1999

ABSTRACT

This study examines how the sediment transport capacity of interrill overland flow varies with stone cover and stone size at two flow intensities. Six series of flume experiments were conducted on two slopes (2° and 10°) with stones of three sizes (28·0, 45·5 and 91·3 mm) serving as roughness elements. Bed sediment size, water discharge and simulated rainfall intensity were the same in all experiments. It was found (1) that transport capacity is positively related to stone size, with the relation becoming stronger as stone cover increases and flow intensity decreases; and (2) that transport capacity is negatively related to stone cover at the high flow intensity and curvilinearly related to stone cover at the low flow intensity. The curvilinear relations are concave-upward with the lowest transport capacities occurring at stone covers between 0·40 and 0·60. The highest transport capacities are found at stone covers of 0 and 1, with the transport capacity being greater at the former stone cover than at the latter. Copyright © 2000 John Wiley & Sons, Ltd.

KEY WORDS: sediment transport; rain-flow transport; flow transport; overland flow; surface roughness; hillslopes

INTRODUCTION

Virtually all physically based soil erosion models developed during the past two decades contain an equation for predicting the sediment transport capacity of overland flow. This is because transport capacity, in conjunction with the inflow of sediment from upslope, controls rates of hillslope erosion and deposition (e.g. Foster and Meyer, 1972; Foster *et al.*, 1995; Smith *et al.*, 1995; Morgan *et al.*, 1998). The ability of present and future models accurately to predict these rates is therefore contingent on the accuracy of the sediment transport equation they employ. The formulation of such an equation for overland flow is complicated by the fact that transport capacity is substantially reduced by surface roughness (Abrahams and Parsons, 1994; Atkinson *et al.*, 2000). Yet there have been few studies of the effect of surface roughness on transport capacity (as distinct from sediment yield) (e.g. Foster, 1982; Foster *et al.*, 1995; Govers and Rauws, 1986). The present study contributes to the limited body of work on this subject by employing stones as roughness elements and examining their effect on the transport capacity of interrill overland flow.

Two studies of the influence of surface stones on the transport capacity of interrill overland flow have recently been published by Abrahams *et al.* (1998) and Li and Abrahams (1999). Abrahams *et al.* (1998) investigated turbulent overland flow in a flume with a sandy bed and slopes of 2·7° to 10°. Experiments were performed both with and without simulated rainfall. Cylinders and miniature ornamental trees as well as stones were used as roughness elements. The stones ranged in cover up to 0·37 and in size up to 91·3 mm. Multiple regression indicated that transport capacity was negatively related to stone cover and positively related to stone size. Li and Abrahams (1999) examined the controls of transport capacity in laminar overland flow in a flume with a sandy bed inclined at 2° to 10°. Experiments were conducted both with and without simulated rainfall using stones as roughness elements. Stone cover ranged up to 0·25 and stone size up to

* Correspondence to: Prof. A. D. Abrahams, Department of Geography, State University of New York at Buffalo, Wilkeson Quad, Box 610023, Buffalo, New York 14261-0023, USA. E-mail: abrahams@geog.buffalo. edu
Contract/grant sponsor: National Science Foundation

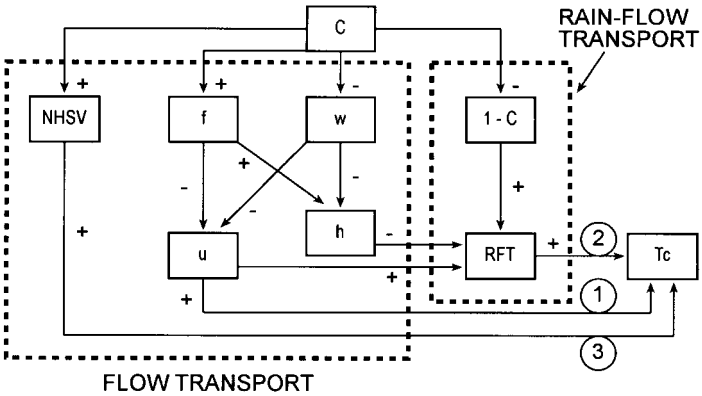

Figure 1. Causal diagram summarizing the pathways (or mechanisms) whereby stone cover affects the sediment transport capacity of interrill overland flow. Flow discharge, slope, sediment size and rainfall intensity (or energy) are constant and so are not included in the diagram. The notation is as follows: C = stone cover, $1–C$ = proportion of the bed exposed to *RFT*, f = resistance to flow, h = flow depth, *NHSV* = number of horseshoe vortices, *RFT* = rain-flow transport, T_c = sediment transport capacity, u = mean flow velocity, and w = flow width

91·3 mm. Multiple regression again revealed that transport capacity was negatively related to stone cover and positively related to stone size.

Abrahams *et al.* (1998) and Li and Abrahams (1999) attributed the negative relation between transport capacity and stone cover to flow resistance increasing with cover, causing flow velocity to decrease and flow depth to increase. Transport capacity then decreases with flow velocity because shear on the bed (as opposed to that on the roughness elements) diminishes. At the same time, as stone cover increases, flow width decreases, causing both flow depth and flow velocity to increase. Thus, stone cover has a negative effect on flow velocity via flow resistance and a positive effect via flow width. Flume experiments conducted at a given discharge and slope (e.g. Figure 4) generally indicate a negative relation between flow velocity and stone cover, which implies that the negative effect of stone cover on flow velocity via flow resistance outweighs the positive effect via flow width.

Figure 1 is a causal diagram that depicts the pathways whereby stone cover controls sediment transport capacity. The transport processes involved are driven by two energy sources: flow energy and raindrop energy. The processes driven by flow energy are collectively termed *flow transport* (FT), whereas those powered by a combination of flow energy and raindrop energy are termed *rain-flow transport* (RFT). RFT refers to the downslope movement of sediment by any mechanism induced by raindrop impact on overland flow (Moss *et al.*, 1979; Moss, 1980). Thus, RFT includes the movement of particles in suspension and by hopping, rolling and sliding so long as the motion is caused (at least in part) by raindrop impact. RFT refers strictly to the transport of sediment; it does not include any form of particle detachment (Moss *et al.*, 1979; Moss, 1980).

As Figure 1 shows, there are three causal pathways linking transport capacity to stone cover. The first involves FT and operates through flow velocity. The second is more complicated, as it involves RFT, which is controlled by flow depth and flow velocity on the one hand and the proportion of the bed exposed to RFT on the other. Flow depth (which has a negative effect) and flow velocity (which has a positive effect) control the efficacy of the process, while the proportion of the bed exposed determines the area over which the process operates. The third causal pathway in Figure 1 is due to horseshoe vortices that form on the stoss side of stones (Bunte and Poesen, 1993, 1994). These vortices generate considerable turbulence which enhances transport capacity by entraining and sustaining sediment in motion. This pathway, like pathway 1, involves FT.

Abrahams *et al.* (1998) and Li and Abrahams (1999) ascribed the positive relation between transport capacity and stone size to three mechanisms. First, a given cover of large stones has a smaller wetted perimeter and, hence, offers less resistance to flow than does the same cover of small stones. Thus, flow velocity increases with stone size, causing transport capacity to increase as shear on the bed (as opposed to

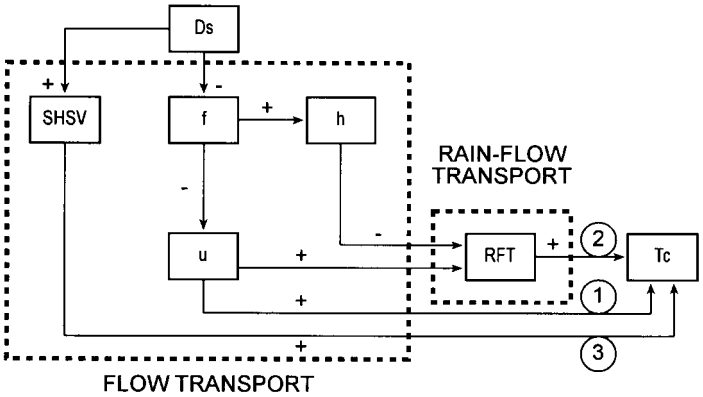

Figure 2. Causal diagram summarizing the pathways (or mechanisms) whereby stone size affects the sediment transport capacity of interrill overland flow. Flow discharge, slope, sediment size and rainfall intensity (or energy) are constant and so are not included in the diagram. The notation is as follows: D_s = stone size and *SHSV* = size of horseshoe vortices. The remaining notation is defined in the caption to Figure 1

that on the roughness elements) increases. Second, flow depth decreases as stone size increases. The increase in velocity and decrease in depth combine to enhance RFT and, hence, transport capacity. Third, large stones deflect greater quantities of water than small ones, thereby forming larger horseshoe vortices which transport larger quantities of sediment. These three causal pathways are depicted in Figure 2, which shows that pathways 1 and 3 involve FT, while pathway 2 involves RFT.

Figures 1 and 2 summarize our knowledge of the ways in which stone cover and size affect transport capacity. Pathways 1 and 2 in Figure 1 give rise to negative relations between stone cover and transport capacity, whereas pathway 3 is expressed by a positive relation between these variables. All three pathways in Figure 2 produce positive relations between stone size and transport capacity. These causal pathways or mechanisms all operate simultaneously. So whether an observed relation between cover and transport capacity is positive or negative depends on which pathways dominate.

The studies by Abrahams *et al.* (1998) and Li and Abrahams (1999) indicate that transport capacity is negatively related to stone cover and positively related to stone size. However, in the former study the maximum stone cover was 0·37, whereas in the latter it was 0·25. Higher stone covers occur in many parts of the world. For example, stone covers are typically 0·50 to 0·70 on desert hillslopes (Abrahams *et al.*, 1986; Abrahams and Parsons, 1991) and may exceed 0·98 on desert pavements (Dury, 1968; Cooke, 1970; Bull, 1991). Accordingly, the present study was undertaken to investigate the relation of transport capacity to stone cover and stone size over the cover range of 0 to 1. In the study, water discharge, rainfall intensity and sediment size are held constant, and stone size, stone cover and slope are varied. Slope is varied as a means of altering flow intensity without changing discharge.

SET-UP AND METHODS

The flume was 5·2 m long and 0·40 m wide with a smooth aluminium floor and plexiglas walls. It consisted of two parts: a lower part, 3·6 m long, which was covered with sand, and an upper steeper part, 1·6 m long. For the experiments the lower part of the flume was inclined at slopes of 2° and 10° and covered with a well sorted sand with a median diameter of 0·74 mm and a density of 2650 kg m^{-3}. Sand of the same size was fed into the upper part of the flume from a vibrating hopper at a rate that was adjusted to maintain the sand cover over the lower part of the flume. Sediment transport capacity T_c (kg m^{-1} s^{-1}) was determined by taking volumetric samples of the water–sediment mixture leaving the flume, calculating the sediment discharge (kg s^{-1}), and dividing this quantity by the flume width W (m).

Water entered the flume by overflowing from a head tank. The inflow, which was measured by a rotameter, was constant at $0{\cdot}135 \times 10^{-3}$ m^3 s^{-1}. The density of the water was assumed to be 1000 kg m^{-3}, while the

kinematic viscosity v ($m^2\ s^{-1}$) was determined from water temperature. During the experiments, simulated rainfall was applied from two Spaco-Lechler full-cone jet nozzles at an intensity of 108 mm h^{-1}. The median raindrop size determined by the flour pellet method was 2·0 mm, and the kinetic energy of the target intensity was 0·65 J $m^{-2}\ s^{-1}$, or 68 per cent of that for a natural rainstorm of the same intensity (Kinnell, 1973). The water discharge from the lower end of the flume Q ($m^3\ s^{-1}$) was computed by adding together the water inflow and the rainfall onto the flume.

At the start of each experiment the water inflow rate was set and the sediment feed was adjusted to this rate. Except for the experiments on the 10° slope when the stone cover was at or near zero, each experiment was allowed to run for about 3 min before any measurements were taken. Two lines of evidence indicate that steady-state conditions existed at that time. First, visual observations suggested that the bed had stabilized. Second, in a special series of measurements, the flume outflow was sampled continuously once the flow had become established. No trend could be detected in the measured sediment concentrations, signifying that adjustment of the sediment transport rate to the flow had occurred before sampling began – that is, within seconds of the flow equilibrating. When the flume was inclined at 10° and had a stone cover at or near zero, the flow began to incise and form rills almost immediately. To minimize the effect of the rilling on the sediment transport rate (since this study is concerned with interrill flow), the flume bed was planed prior to each experiment and measurements were taken as soon as practicable (typically within 30 to 60 s) after the flow was established.

The roughness elements consisted of three groups of stones collected from a local river bed. The stones in the three groups were similar in shape (with a mean shape factor $c/(ab)^{1/2}$ ranging from 0·566 to 0·605) and in roundness (with all groups having a modal roundness index of 5 on (Powers' 1953) six-point scale) but different in size. Because the stones were randomly placed in the flume with their a–b planes parallel to the bed, stone size was measured by $(a + b)/2$. The median values of this index D_s were 28·0, 45·5 and 91·3 mm for the three groups. Stone cover C was determined by placing a 50 mm by 50 mm grid over the flume and computing the proportion of the grid intersection points underlain by stones. Because the stones were partly buried in the sand with their c axes perpendicular to the bed, at high values of C the 28·0 mm stones were almost completely covered by the flow, the 45·5 mm stones were mostly covered, and the smallest of the 91·3 mm stones were partly covered.

The mean flow velocity u (m s^{-1}) was determined by a salt tracing technique described elsewhere (Li and Abrahams, 1997). For the experiments with the 91·3 mm stones, the mean flow width w (m) was calculated from $w = W(1 - C)$ and the mean flow depth h (m) from $h = Q/uw$. Where the stones were partly inundated, the equivalent of C was the area of the stones protruding through the flow divided by the area of the bed. However, the area of protruding stones was not measured. As this area was needed to calculate w and h, these hydraulic variables could not be computed for most of the experiments with the 28·0 mm and 45·5 mm stones, and so neither could the flow Reynolds number $Re = 4uh/v$ or the Froude number $F = u/(gh)^{1/2}$. For the experiments with the 91·3 mm stones, $1627 \leq Re \leq 14\ 882$ and $0{\cdot}148 \leq F \leq 0{\cdot}886$ on the 2° slope, and $1734 \leq Re \leq 8682$ and $0{\cdot}392 < F \leq 1{\cdot}147$ on the 10° slope.

RESULTS

Six series of experiments were undertaken, one for each combination of the three stone sizes D_s (28·0, 45·5 and 91·3 mm) and two slopes (2° and 10°). In each series C varied from 0 up to about 0·90, the latter proportion being the highest that could be achieved given the rounded corners of the stones. The results of these experiments are presented in Figure 3, which reveals the following.

(1) On the 2° slope the T_c–C relations for all three D_s have concave-upward trends. The minima of these relations lie within the range $0{\cdot}40 < C < 0{\cdot}60$, whereas the maxima occur at $C = 0$. In other words, surface stones regardless of their cover cause T_c to decline below its value for the plane bed.
(2) On the 10° slope the T_c–C relations for all three D_s are negatively sloping.
(3) On both the 2° and the 10° slopes, T_c tends to increase with D_s. The dependency of T_c on D_s increases as slope decreases and as C increases.

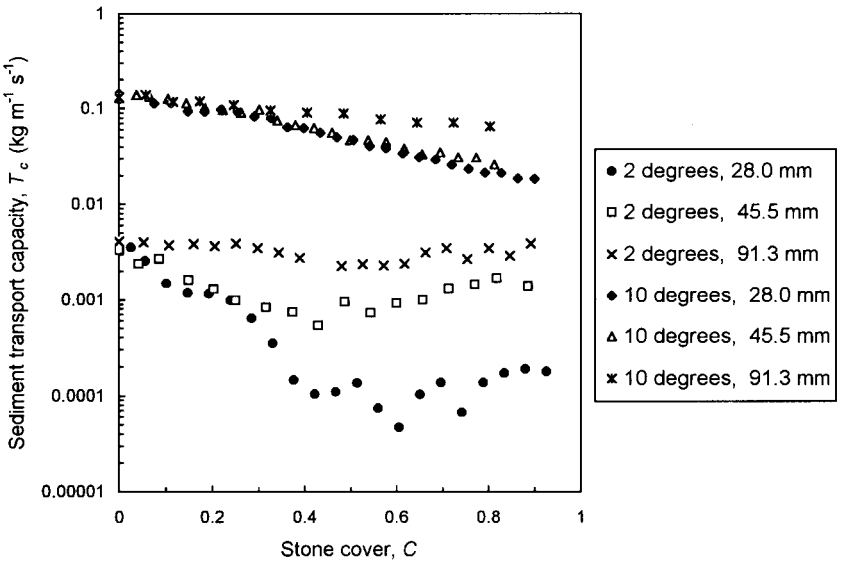

Figure 3. Graph of sediment transport capacity against stone cover. The key indicates the slope and stone size used in each series of experiments

DISCUSSION

Effect of stone cover

The first and second results may be explained with the aid of the causal diagram in Figure 1. Bearing in mind that flow intensity increases with slope, Figure 1 implies that at relatively high flow intensities (high slopes) where the T_c–C relation is negatively sloping, C affects T_c predominantly by means of pathways 1 and 2. The same is true at low flow intensities (low slopes) where C is small and the T_c–C relation is negatively sloping. However, the two pathways are not equally important. The proclivity of the flow to incise where $C \cong 0$ on the 10° slope indicates that FT dominates RFT and, hence, that the first pathway is more important than the second. In contrast, the inability of flow to incise when $C \cong 0$ on the 2° slope signifies that RFT dominates FT and, hence, that the second pathway is more important than the first.

At low flow intensities where C is large and the T_c–C relation is positively sloping, C influences T_c mainly via the third pathway. A positive slope exists where C is large because large numbers of stones generate large numbers of horseshoe vortices which counteract the tendency of pathways 1 and 2 to produce a negative slope.

In Figure 4 the mean flow velocity u is plotted against C for the three stone sizes and two flow intensities (slopes). For the high intensity flows (10° slope), the u–C plots are remarkably similar to the T_c–C plots (Figure 3), suggesting that u is a major control of T_c. Given that RFT is less effective than FT on 10° slopes, it may be inferred that u affects T_c principally via pathway 1.

Although the u–C and T_c–C plots are similar for the low-intensity flows (2° slope), there are two differences that deserve comment. First, the u–C plots do not have positively sloping limbs comparable to the T_c–C plots. This observation is in accordance with the above suggestion that the positively sloping limbs on the T_c–C plots are largely the product of pathway 3. The levelling off of the u–C graphs for the 28·0 mm and 45·5 mm stones where $C > 0{\cdot}6$ is presumably due to the gradual inundation of these stones as C increases.

Second, in Figure 4b the values of u for the 28·0 mm stones plot above those for the 45·5 mm stones, whereas in Figure 3 the values of T_c for the 28·0 mm stones plot below those for the 45·5 mm stones. Furthermore, the differences between these plots increase with C. These findings may be explained as follows: (1) a larger proportion of the flow passes over the 28·0 mm stones than over the 45·5 mm ones; (2)

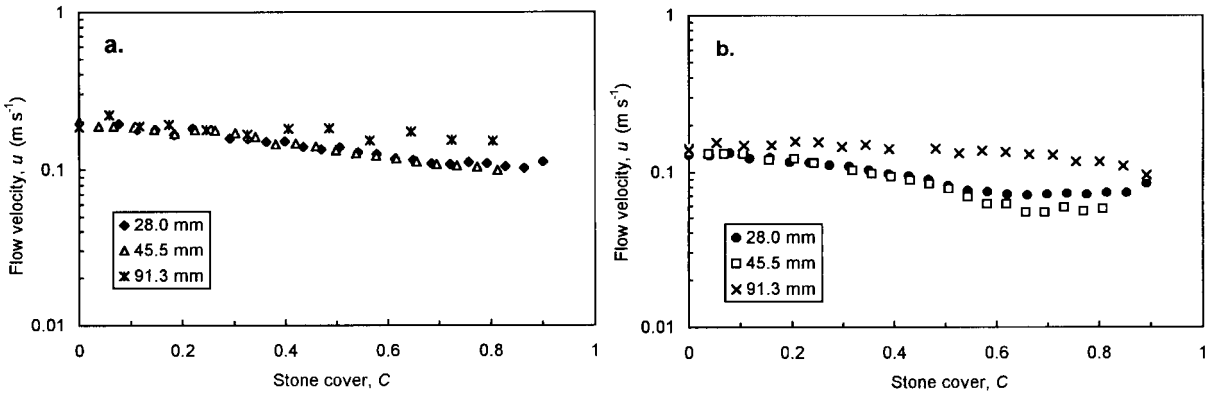

Figure 4. Graphs of mean flow velocity against stone cover for (a) a 10° bed slope and (b) a 2° bed slope

the difference between the proportions increases with C; (3) the skimming flow passing over the stones is faster than that passing between them; and (4) the former flow has a lower transport capacity than the latter because the former flow is passing over stones which do not contribute sediment to the flow.

Assuming it is possible to fit stones together to form a mosaic with $C = 1$ so that the entire flow passes over the stones, it is interesting to speculate on the value of T_c relative to its value where $C = 0$. Although the flow will not be able to entrain sediment lying beneath the stones where $C = 1$, it will be able to transport sediment supplied from upslope. Thus, T_c will be greater than zero, but at the same time it will be less than its value for the corresponding sediment-covered bed with $C = 0$. This assertion is supported by two lines of reasoning which rest on the assumption that the stone mosaic is not completely covered with sediment (otherwise it would be indistinguishable from the case where $C = 0$). First, the stone mosaic will almost certainly have a rougher surface than the sediment-covered bed; thus, the flow velocity will be less and so will T_c. Second, both FT and RFT will dissipate energy on the bare stone surfaces that will not contribute to sediment transport, so T_c will be diminished. The assertion that T_c is less where $C = 1$ than where $C = 0$ is consistent with Figure 3, which shows that maximum T_c always occurs at $C = 0$.

Effect of stone size

The third result reported above may be understood in terms of the causal diagram in Figure 2. The tendency for T_c to increase with D_s in Figure 3 is consistent with and may be attributed to the three causal pathways in Figure 2. However, while this causal diagram accounts for the dependency of T_c on D_s, it is unable to explain why the dependency increases as slope decreases and C increases. A reasonable answer to this question is provided by the literature on scour around bridge piers. Melville (1997) found that scour depth is dependent on pier width b and flow depth h, but the relative strengths of these dependencies vary with b/h. For relatively deep flows (where $b/h < 0{\cdot}7$) scour depth is positively related to b and independent of h. As flow depth decreases, scour depth becomes less dependent on b and more dependent on h until for relatively shallow flows (where $b/h > 5$) scour depth is positively related to h and independent of b. Ettema (1980) explained that for shallow flows, the surface roller that forms upstream of a bridge pier interferes with the scour action of the horseshoe vortex, which rotates in the opposite direction. With increasing flow depth, the interference diminishes and eventually becomes insignificant.

Assuming that b is equivalent to D_s and that the ability of a horseshoe vortex to transport sediment is proportional to its size which, in turn, is proportional to its depth of scour, the above relations for pier scour may be used to explain why the dependency of T_c on D_s increases as slope decreases and C increases. Recalling that discharge is constant in the present experiments, for a given C the flow on the 2° slope is deeper than that on the 10° slope. Thus, it may be inferred from the pier scour relations that the dependency of T_c on D_s will increase with flow depth and, hence, be stronger on the 2° slope than on the 10° slope. Figure 3 shows

that this is indeed the case. Likewise, on a given slope flow depth increases with C. It follows from the pier scour relations that as flow depth increases, T_c should become increasingly dependent on D_s. This is clearly evident in Figure 3 for both the 2° and the 10° slopes.

CONCLUSION

This study examines how the sediment transport capacity of interrill overland flow varies with stone cover and stone size at two flow intensities. Transport capacity is positively related to stone size, with the relation becoming stronger as stone cover increases and flow intensity decreases. The positive relation is attributed to flow resistance decreasing and the size of horseshoe vortices increasing as stone size increases. The variation in the strength of the relation is explained by referring to the literature on pier scour which implies that the dependency of transport capacity on stone size increases as flow depth increases, and flow depth increases as stone cover increases and slope decreases.

Transport capacity is negatively related to stone cover at the high flow intensity and curvilinearly related to it at the low flow intensity. The curvilinear relations are concave-upward with the lowest transport capacities at stone covers between 0·40 and 0·60. The highest transport capacities are found at stone covers of 0 and 1, with the transport capacity being greater at the former stone cover than at the latter because the bed is smoother at the former and the sediment cover is incomplete at the latter. Positively sloping transport capacity–stone cover relations are attributed to horseshoe vortices increasing in number with stone cover, whereas negatively sloping relations are ascribed (1) to flow resistance increasing with stone cover causing flow velocity to decline, (2) to flow depth increasing with stone cover causing RFT to diminish, and (3) to the proportion of the bed exposed to RFT decreasing as stone cover increases.

ACKNOWLEDGEMENTS

This research was supported by the Geography and Regional Science and the Jornada Long-Term Ecological Research (LTER) programs of the National Science Foundation. We are grateful to Sean Coughlin and Nicole Love for their assistance with the experiments and to P.I.A. Kinnell for helpful comments on the manuscript.

REFERENCES

Abrahams, A. D., Parsons and A. J. 1991. Resistance to overland flow on desert pavement and its implications for sediment transport modeling. *Water Resources Research,* **27**, 1827–1836.

Abrahams, A. D. and Parsons, A. J. 1994. Hydraulics of interrill overland flow on stone-covered desert surfaces. *Catena,* **23**, 111–140.

Abrahams, A. D, Parsons, A. J. and Luk, S-H. 1986. Resistance to overland flow on desert hillslopes. *Journal of Hydrology,* **88**, 343–363.

Abrahams, A. D., Li, G., Krishnan, C. and Atkinson, J. F. 1998. Predicting sediment transport by interrill overland flow on rough surfaces. *Earth Surface Processes and Landforms,* **23**, 481–492.

Atkinson, J. F., Abrahams, A. D., Krishnan, C. and Li, G. 2000. Shear stress partitioning and sediment transport by overland flow. *Journal of Hydraulic Research*, in press.

Bull, W. B. 1991. Geomorphic Responses to Climatic Change. Oxford University Press: Oxford.

Bunte, K. and Poesen, J. W. 1993. Effects of rock fragment covers on erosion and transport of noncohesive sediment by shallow overland flow. *Water Resources Research,* **29**, 1415–1424.

Bunte, K. and Poesen, J. W. 1994. Effects of rock fragment size and cover on overland flow hydraulics, local turbulence and sediment yield on an erodible soil surface. *Earth Surface Processes and Landforms,* **19**, 115–135.

Cooke, R. U. 1970. Morphometric analysis of pediments and associated landforms in the western Mojave Desert, California. *American Journal of Science,* **269**, 26–38.

Dury, G. H. 1968. Gibber. In Encyclopedia of Geomorphology, Fairbridge, R. W. (ed.). Reinholt: New York: 424.

Ettema, R. E. 1980. Scour at bridge piers. Report No. **236**. School of Engineering, The University of Auckland; New Zealand.

Foster, G. R. 1982. Modeling the erosion process. In Hydrologic Modeling of Small Watersheds, Hann, C. T. (ed.). American Society of Agricultural Engineers: St. Joseph, Mich.; 297–380.

Foster, G. R. and Meyer, L. D. 1972. A closed-form soil erosion equation for upland areas. In Sedimentation, Shen, H. W. (ed.). H.W. Shen: Fort Collins, Colo.; 12-1–12-19.

Foster, G. R., Flanagan, D. C., Nearing, M. A., Lane, L. J., Risse, L. M. and Finkner, S. C. 1995. Hillslope erosion component. In USDA-Water Erosion Prediction Project Hillslope Profile and Watershed Model Documentation. NSERL Report **10**. National Soil Erosion Research Laboratory: West Lafayette, Ind.; 11·1–11·12.

Govers, G. and Rauws, G. 1986. Transporting capacity of overland flow on plane and irregular beds. *Earth Surface Processes and Landforms* **11**, 515–524.

Kinnell, P. I. A. 1973. The problem of assessing the erosive power of rainfall from meteorological observations. *Soil Science Society of America Proceedings,* **37**, 617–621.
Li, G. and Abrahams, A. D. 1997. Effect of saltating sediment load on the determination of the mean velocity of overland flow. *Water Resources Research,* **33**, 341–347.
Li, G. and Abrahams, A. D. 1999. Controls of sediment transport capacity in laminar interrill flow on stone-covered surfaces. *Water Resources Research,* **35**, 305–310.
Melville, B. W. 1997. Pier and abutment scour: integrated approach. *Journal of Hydraulic Engineering* **123**: 125–136.
Morgan, R. P. C., Quinton, J. N., Smith, R. E., Govers, G., Poesen, J. W. A., Auerswald, K., Chisci, G., Torri, D. and Styczen, M. E. 1998. The European Soil Erosion Model (EUROSEM): a dynamic approach for predicting sediment transport from fields and small catchments. *Earth Surface Processes and Landforms,* **23**, 527–544.
Moss, A. J. 1980. Thin-flow transportation of solids in arid and non-arid areas: a comparison of processes. International Association of Hydrological Sciences Publication, **128**, 435–445.
Moss, A. J,. Walker, P. H. and Hutka, J. 1979. Raindrop-stimulated transportation in shallow water flows: an experimental study. *Sedimentary Geology,* **22**, 165–184.
Powers, M. C. 1953. A new roundness scale for sedimentary particles. *Journal of Sedimentary Petrology,* **23**(2), 117–119.
Smith, R. E., Goodrich, D. C., Woolhiser, D. A. and Unkrich, C. L. 1995. KINEROS – A kinematic runoff and erosion model. In Computer Models of Watershed Hydrology, Singh, V. P. (ed.). Water Resources Publications: Highlands Ranch, Colo.; 697–732.

